PERGAMON

Renewable Energy 28 (2003) 139–152

RENEWABLE ENERGY

www.elsevier.com/locate/renene

Technical note

Development of an integrated data-acquisition system for renewable energy sources systems monitoring

Eftichios Koutroulis *, Kostas Kalaitzakis

Department of Electronics and Computer Engineering, Technical University of Crete, GR-73100, Chania, Greece

Received 1 October 2001; accepted 16 November 2001

Abstract

Data-acquisition systems are widely used in renewable energy source (RES) applications in order to collect data regarding the installed system performance, for evaluation purposes. In this paper, the development of a computer-based system for RES systems monitoring is described. The proposed system consists of a set of sensors for measuring both meteorological (e.g. temperature, humidity etc.) and electrical parameters (photovoltaics voltage and current etc.). The collected data are first conditioned using precision electronic circuits and then interfaced to a PC using a data-acquisition card. The LABVIEW program is used to further process, display and store the collected data in the PC disk. The proposed architecture permits the rapid system development and has the advantage of flexibility in the case of changes, while it can be easily extended for controlling the RES system operation. © 2002 Elsevier Science Ltd. All rights reserved.

Keywords: Renewable energy sources; Data-acquisition system; Microcomputer; Sensors; LABVIEW

1. Introduction

The rapid evolution of renewable energy sources (RESs) during the last two decades resulted in the installation of many RES power systems all over the world. A disadvantage of RES systems is that the installation cost is still high, so their design

* Corresponding author.

PII: S0960-1481(01)00197-5

optimization is desirable. However, such an effort requires detailed knowledge of meteorological data of the site where the system will be installed and operational results from similar systems, if available. Many data-acquisition systems have been developed in order to collect and process such data, as well as monitor the performance of RES systems under operation, in order to evaluate their performance [1–3].

A data-acquisition system used for monitoring the performance of both photovoltaic battery charging [4] and water-pumping systems [5] is shown in Fig. 1(a). An A/D converter interfaced to a microcontroller-based unit records a set of sensors' signals, while the collected data are stored in a local EPROM. The data collected by the microcontroller are transmitted to a PC, with an RS-232 serial connection, where they are stored for further processing. The same architecture has been implemented in [6–8] for solar irradiation and ambient temperature measurements. In all the above-mentioned cases, Windows or MS-DOS based software was developed specifically for each application, in order to process and display the collected data on the PC, but this approach is not flexible to changes, e.g. the addition of new sensors.

A different approach has been proposed in [9], shown in Fig. 1(b). A commercial data-logging unit has been used to measure a set of meteorological and operational parameters of a hybrid photovoltaic–diesel system. The collected data are transmitted to a PC through an RS-232 serial interface, where they are processed using the LABVIEW data acquisition software. However, a data logging unit lacks flexibility compared with a data-acquisition card approach, while, in addition, it cannot be used for RES system control.

A common characteristic of the design methods described above is that a microcontroller-based data-logging unit is used to measure the signals of interest and interface the collected data to a PC through an RS-232 serial interface. However, serial data transmission limits the system performance if an advanced control capability is desired.

In this paper, a computer-based data-acquisition system for monitoring both meteorological data and RES system operational parameters is proposed. A block diagram of the proposed system is shown in Fig. 1(c). A set of sensors are used to measure atmospheric and soil conditions, as well as quantities regarding the energy produced by the hybrid photovoltaic/wind generator power system, such as the photovoltaic array voltage and current, the wind generator speed etc. The sensor signals are first filtered and amplified using precision electronic circuits and then are interfaced to a PC, through the PCI bus, using a commercially available data-acquisition card. The collected data are further processed, displayed on the monitor and stored in the disk using the LABVIEW software. This method has the advantages of rapid data-acquisition system development and flexibility in the case of changes, while it can be easily extended to control the RES system operation. Also, the LABVIEW provides an easy-to-use graphical environment that permits the system operators to process easily the collected data, using complex data-processing algorithms, without detailed knowledge of the data-acquisition system design [10]. The proposed data-acquisition system has been interfaced to a pilot low-power RES system just for test purposes, but this does not limit its use on large power capacity RES plants, which is the main objective of such monitoring and control systems.

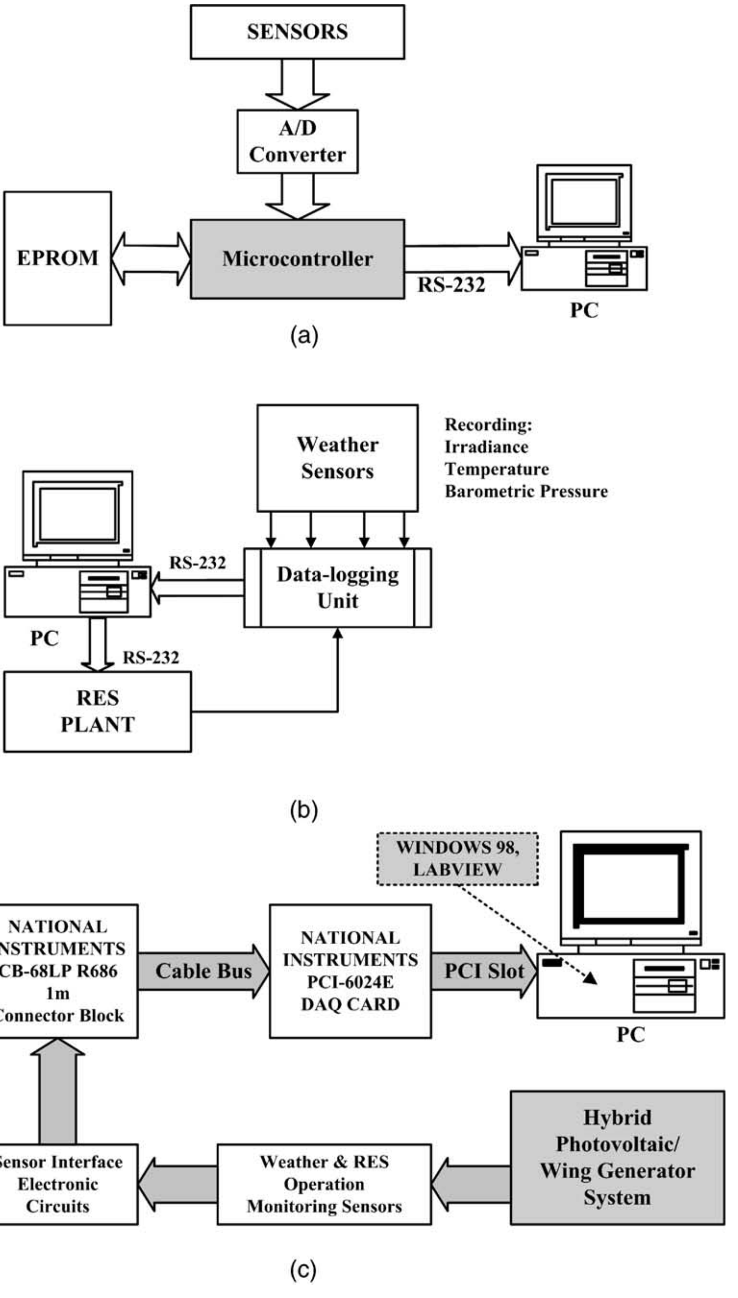

Fig. 1. Data-acquisition architectures for RES systems: (a) a microcontroller-based system, (b) a data-logging unit connected to a PC and (c) the proposed arrangement block diagram.

This paper is organized as follows: an analysis of the sensors and the electronic circuits developed is presented in Section 2, the data collection and processing interfaces are described in Section 3 and the experimental results of the proposed design application in an operating hybrid RES system are given in Section 4.

2. The sensors and the interface circuits

A block diagram of the RES system under consideration is shown in Fig. 2. The positions of the sensors used are also indicated in the figure. The power plant consists of two photovoltaic (PV) arrays of 450 and 300 W, respectively, and a 2 kW permanent magnet (PM) wind generator (W/G). Both the W/G and one of the PV arrays are used to charge a 24 V battery stack, by means of appropriate battery chargers. A DC/AC inverter is used to supply the load, which in this case is the lamp array of a parking lot. The second PV array is interconnected to the electric grid through a grid-connected-type inverter. The size of the above RES plant is experimental, but

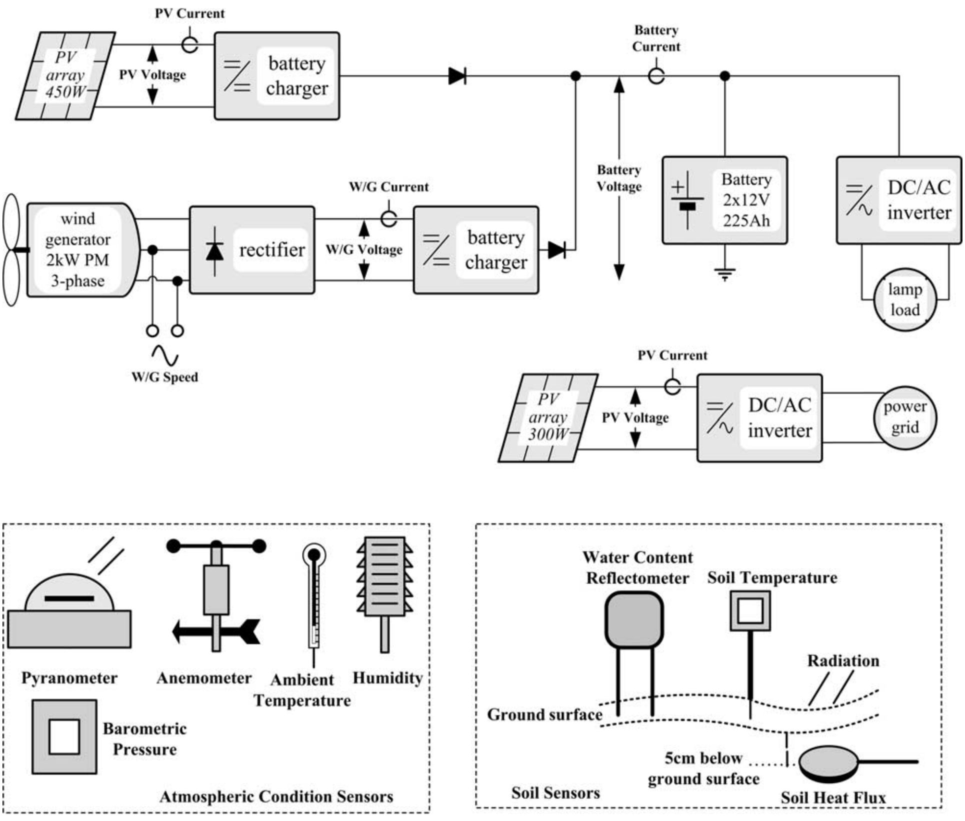

Fig. 2. The RES system block diagram and the sensors used.

the proposed data-acquisition system can be interfaced to larger power capacity RES plants, where the PC power consumption is negligible compared with that generated by the RES system.

The voltages of both PV arrays and the W/G are measured with voltage dividers connected to an AD625 precision instrumentation amplifier [Fig. 3(a)].

The amplifier output voltage is given by the following equation:

$$V_o = \frac{R_F}{R + R_F} V_{in} \tag{1}$$

where V_o is the output voltage, V_{in} is the measured PV or W/G voltage and R, R_F are the voltage divider resistances.

In RES systems equipped with batteries as storage units, the battery service time depends on the estimated state of charge, which is highly sensitive to the current measurement errors. In such cases, if the battery charge monitoring is based on amp-hour measurements using Hall-effect sensors [11], a circuitry improving the measurement accuracy is essential, as explained below.

All currents are measured with Honeywell Microswitch CSLA1CF type Hall-effect sensors. The non-intrusive method of measurement and the very low power loss are among the advantages of this type of sensor. A disadvantage is that the zero current offset voltage has a temperature coefficient of ±0.05%/°C relative to the offset at 25°C. The measurement of currents as high as 100 A dictates the use of a single wire turn wound around the magnetic core, causing relatively high errors when measuring low currents, due to the sensor temperature coefficient. Thus, the development of a temperature compensation arrangement is necessary. The Hall-effect sensors compensation circuit developed is depicted in Fig. 3(b). The forward voltage temperature drift of a small signal diode balances the Hall-effect sensor offset voltage temperature drift. The Hall-effect sensors compensation circuit tested in the laboratory features a temperature coefficient of $\mathrm{d}V_H/\mathrm{d}T = -0.8\ \mathrm{mV/°C}$, while the compensation diode has a coefficient of $\mathrm{d}V_D/\mathrm{d}T = -2.3\ \mathrm{mV/°C}$, where V_H is the Hall-effect sensor output voltage, V_D is the compensation diode voltage and T is the temperature.

The instrumentation amplifier output voltage V_c is given by the following equation:

$$V_c = (V_H - V_{r1}).G_1 + (V_{r2} - V_D).G_2 \tag{2}$$

where G_1, G_2 are the amplifier A1, A2 gains, respectively, and V_{r1}, V_{r2} are reference voltages.

Initially, both potentiometers are trimmed so that $V_H = V_{r1}$ and $V_D = V_{r2}$. Then, the amplifier gain G_1 is calculated as:

$$G_1 = \frac{V_{c,max}}{S_H.I_{max}} \tag{3}$$

where $V_{c,max}$ is the desired maximum output voltage of amplifier A1, S_H is the sensor sensitivity (V/A) and I_{max} is the maximum measured current.

The amplifier A2 gain is calculated differentiating Eq. (2), with respect to temperature, and setting $\mathrm{d}V_c/\mathrm{d}T = 0$, resulting in:

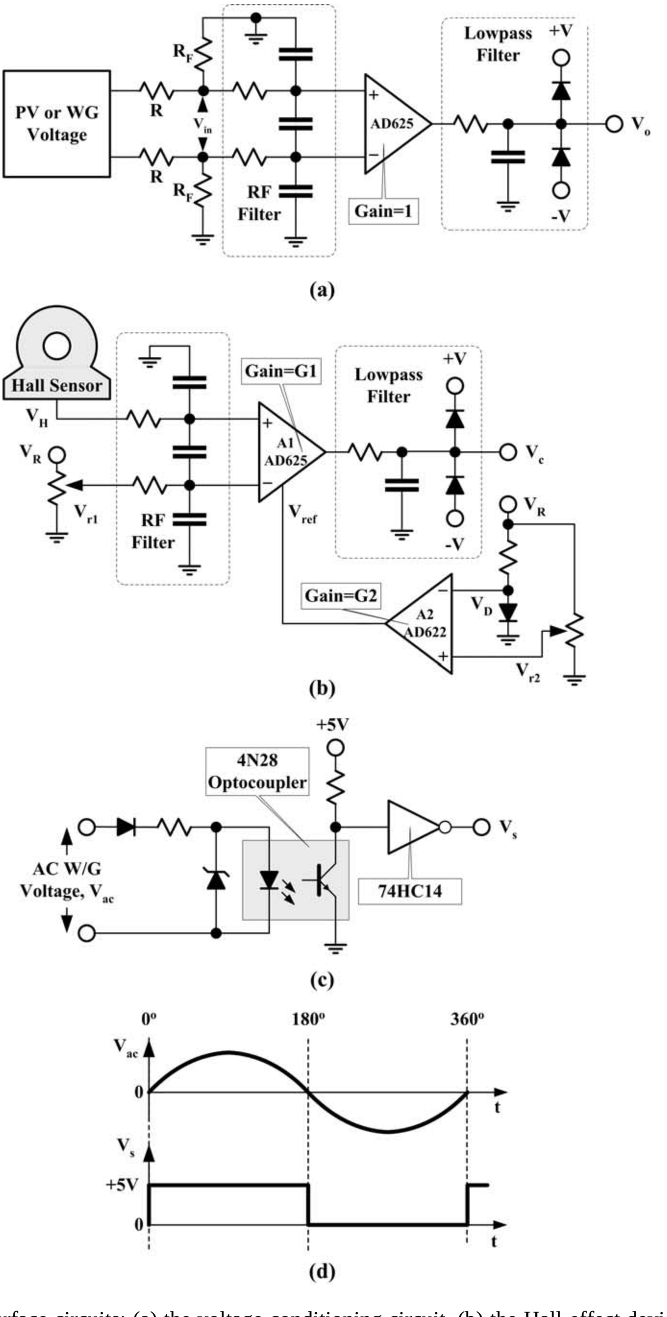

Fig. 3. The interface circuits: (a) the voltage conditioning circuit, (b) the Hall-effect device conditioning and temperature compensation circuits, (c) the W/G speed measurement circuit and (d) the associated waveforms of the circuit shown in (c).

$$G_2 = \frac{dV_H/dT}{dV_D/dT} \cdot G_1 \tag{4}$$

The W/G rotational speed is measured using the circuit shown in Fig. 3(c). As shown in Fig. 3(d), the sinusoidal voltage between two phases of the W/G (V_{ac}) is transformed into a TTL level digital signal (V_s) with frequency (f_{WG}) proportional to the W/G speed. This digital signal is connected to one of the data-acquisition card counter inputs and the W/G speed is computed by means of the data-collection software, as explained in the next section.

All other atmospheric and soil condition sensor signals are amplified differentially using AD625 type instrumentation amplifiers, while the amplifier outputs are connected to the data-acquisition card analog input channels through low-pass RC filters and protection diodes, as shown in Fig. 4.

The ambient temperature and humidity are measured using the Rotronic MP100A type hygrometer, while the barometric pressure and the global irradiation are measured using the Delta-T Devices BS4 type barometer and the GS1 type pyranometer, respectively. The wind speed and direction are measured with the Vector Instruments A100R type anemometer and the W200P type wind vane, respectively. The wind speed signal is connected to a counter input of the data-acquisition card (Fig. 4).

The soil temperature is measured with a PT100 Platinum resistance RTD type sensor and the soil heat flux is measured with a Hukseflux HFP01 type heat flux plate. The soil volumetric water content is measured with the Campell Scientific CS615-L type water content reflectometer. Its output voltage period is proportional

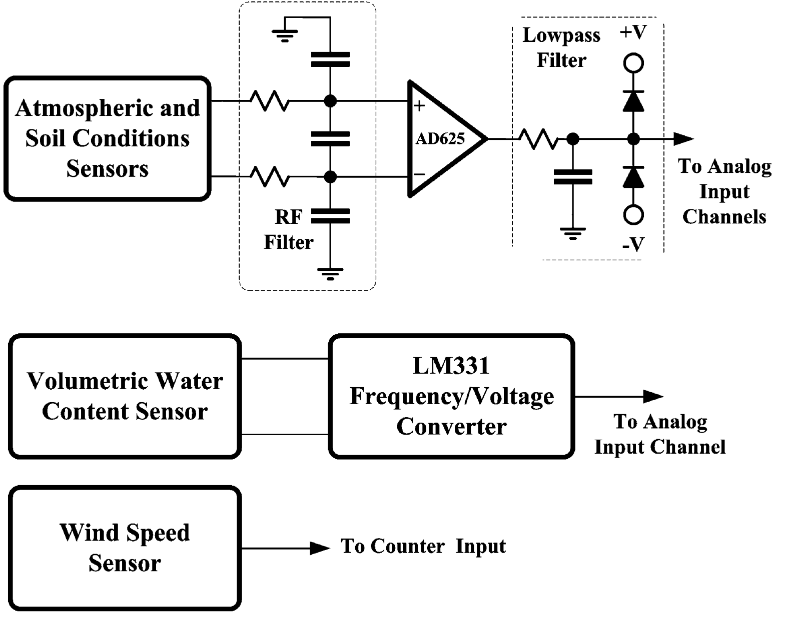

Fig. 4. Block diagrams of the atmospheric and soil condition sensor interface circuits.

to the soil volumetric water content and is converted to an analog signal with the LM331 precision frequency-to-voltage converter (Fig. 4).

3. The data collection and processing interfaces

The data-acquisition system uses the National Instruments PCI-6024E type DAQ card installed in a PC. All instrumentation amplifier outputs and the digital signals are connected to the card through the external CB-68LP R686 connector block.

The DAQ card has the following operational characteristics:

- 16 single ended or eight differential analog input channels (software selectable per channel) with a ±10 V operating range;
- a successive approximation A/D converter with a 12-bit accuracy and a 200 kS/s maximum sampling rate;
- two analog output channels with 12-bit accuracy;
- eight digital input/output channels; and
- two up/down timer/counters.

The data-acquisition card is controlled by a properly developed interface, using the LABVIEW software, running on the PC. It consists of two parts: (a) a graphical environment with components such as displays, buttons and charts in order to provide a convenient-to-use environment for the system operator, and (b) the program code, which is in block-diagram format and consists of built-in virtual instruments (VIs), performing functions such as analog channel sampling, mathematical operations, file management etc. The LABVIEW software runs under the Windows 95/98/NT/2000 operating system and it requires a Pentium processor, a minimum RAM of 32 MB and 60 MB of disk storage space.

The block diagram of the developed LABVIEW program is illustrated in Fig. 5. Initially, all analog signals are sequentially sampled and the input voltage data are calibrated to correspond to physical units. The calibration equations have the general form:

$$y_i = a_i.x_i + b_i \tag{5}$$

where y_i is the ith sensor output in physical units, x_i is the ith sample and a_i, b_i are calibration constants.

The frequency of the anemometer digital output signal is used for calculation of the wind speed, forming the corresponding LABVIEW built-in VI. The relation for the conversion of frequency to wind speed is the following:

$$v_{\mathrm{lin}} = \frac{N_{\mathrm{a}}}{D} = \frac{60 \times f_{\mathrm{a}}}{D} \tag{6}$$

where v_{lin} is the calculated speed (m/s), N_{a} are the anemometer revolutions per minute (rpm), D is a conversion constant given by the anemometer manufacturer and equal to 47.7 rpm/m/s and f_{a} is the measured frequency (Hz).

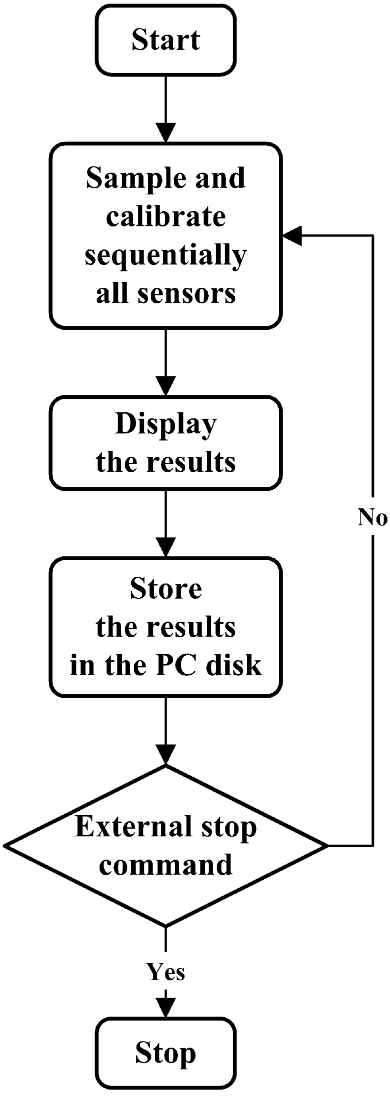

Fig. 5. The LABVIEW measurement program flowchart.

The wind speed is further corrected using the R30 Rotor calibration data. The corresponding correction factor F is calculated by interpolation, using a look-up table and the wind speed v_{lin} calculated in Eq. (6). The correct wind speed v_a (m/s) is then derived from the following equation:

$$v_a = \frac{v_{lin}}{F} \quad (7)$$

Since the wind speed anemometer is located on a mast at a height of 12 m, while the W/G turbine is at 15 m, the following equation is used to calculate the wind speed at the height of the turbine:

$$v_{WG} = v_a \left(\frac{h_{WG}}{h_a} \right)^P \tag{8}$$

where v_a is the measured speed at the height of the anemometer h_a, v_{WG} is the estimated wind speed at the turbine height h_{WG} and $P = 1$ is the stability constant.

The W/G rotational speed N_{WG} is calculated from the corresponding digital signal frequency, as described in the previous section, using the following equation:

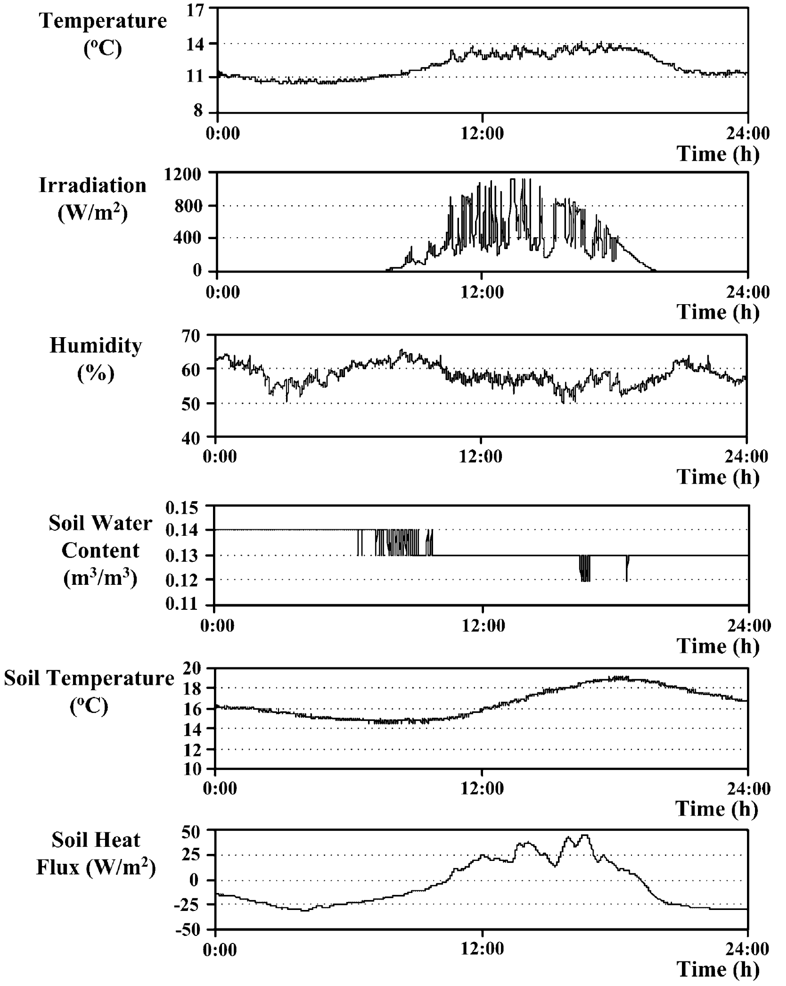

Fig. 6. Atmospheric and soil condition measurements for a specific day.

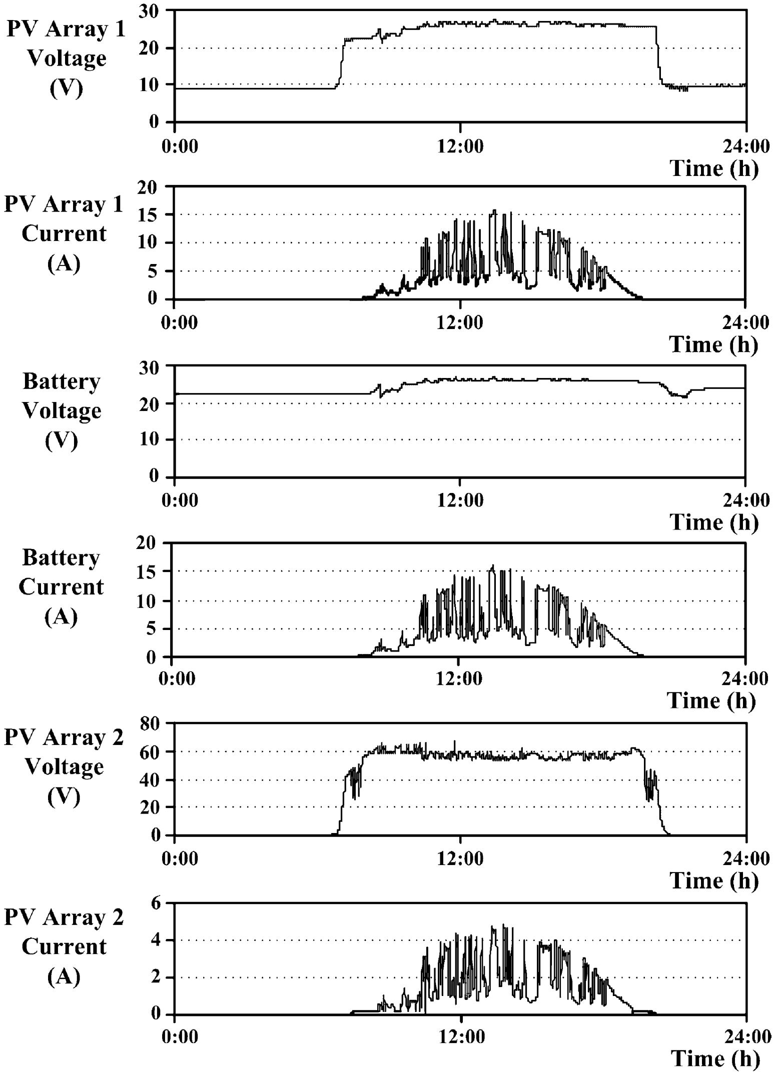

Fig. 7. PV and battery voltage and current measurements for a specific day.

$$N_{WG} = \frac{f_{WG}}{p} \times 60 \quad (9)$$

where N_{WG} is the rotational speed (rpm), f_{WG} is the measured frequency (Hz) and $p = 8$ is the number of the W/G pole pairs.

When the calibration procedure is completed, the calculated values are displayed on the monitor. Also, the measurements performed every 1 min are stored on the PC hard disk, in files named with the current date. These files contain the exact time

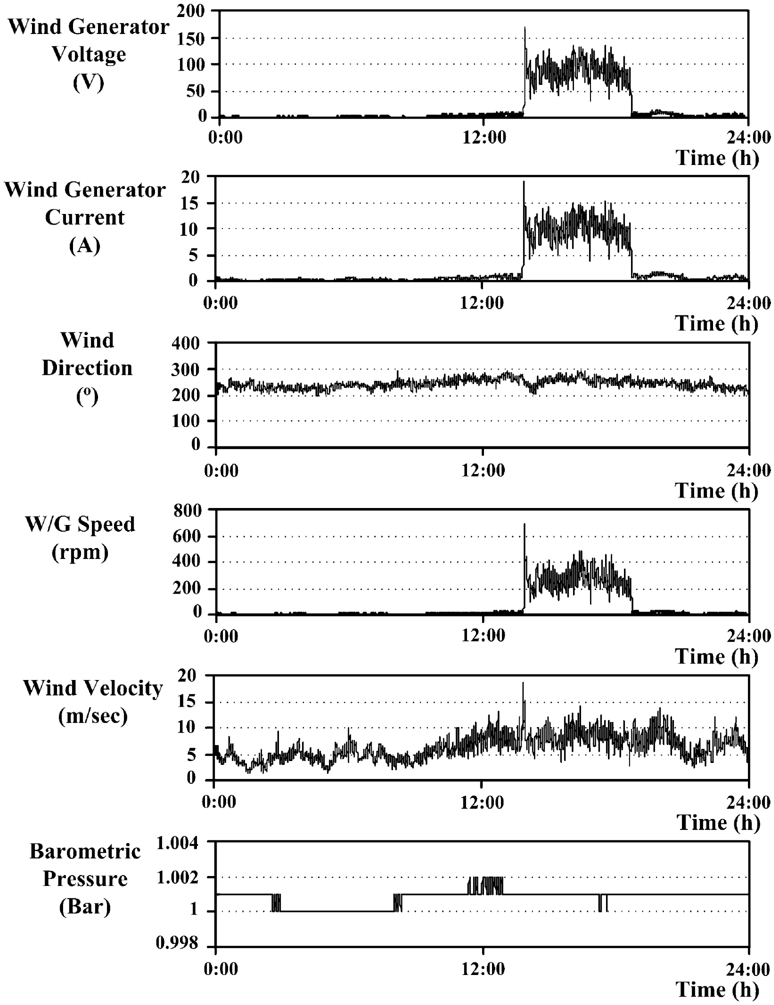

Fig. 8. Wind speed, wind direction, barometric pressure and W/G speed, voltage and current measurements for a specific day.

of the measurement along with each measured parameter identification and value. The above described LABVIEW program runs continuously.

4. The experimental results

The monitoring system together with the power system described above is installed in a small house close to the RES. The geographical location of the installation is approximately: latitude: 35.53° (35° 31′ 48″ N); longitude: 24.06° (24° 03′ 35″ E); altitude: 150 m (approx.) above sea level.

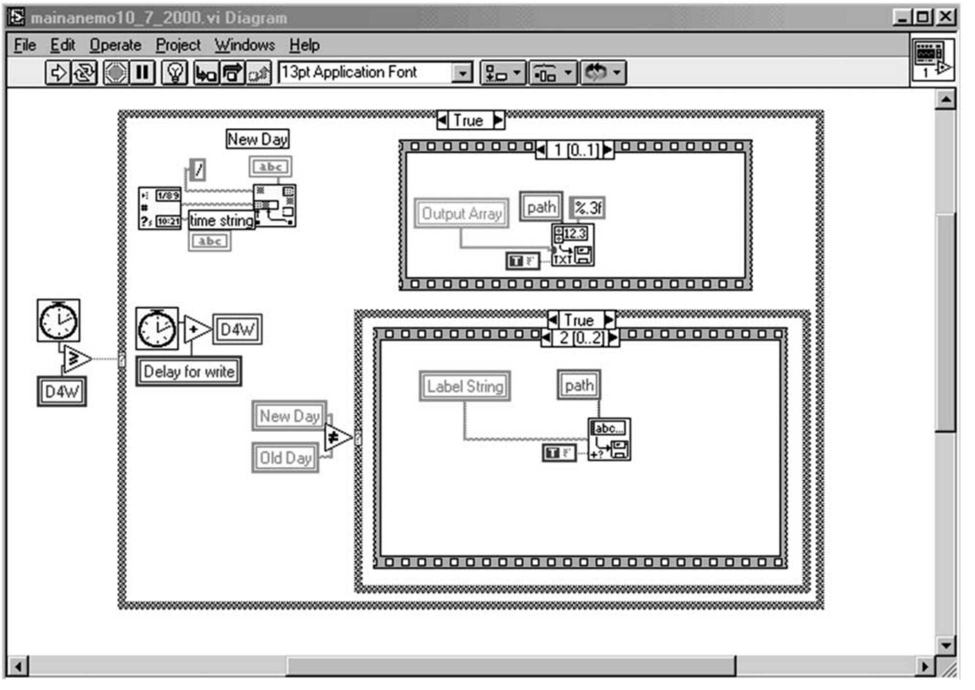

Fig. 9. Part of the developed LABVIEW program code.

The measurements of all sensors described in Section 2, collected in a specific day, are illustrated in Figs. 6–8. A part of the LABVIEW program code is shown in Fig. 9.

The Hall-effect sensors used are wound with a single turn, giving a sensitivity of 26 mV/A. The temperature compensation circuit, described in Section 2, was tested in the range of 20–30°C. The zero current temperature drift measured is less than 3% of the sensor sensitivity, while if no temperature compensation is used, then the maximum zero current temperature drift, in the same temperature range, would be about 15% of the sensor sensitivity. These results verify the accuracy improvement of the Hall-effect sensor current measurements by the compensation circuit.

5. Conclusions

Data-acquisition systems are used in RES systems in order not only to measure the meteorological conditions, but also to collect data regarding the system performance for evaluation purposes. Most present data-acquisition systems collect the data of interest and store them in a local memory until the system operator downloads them to a computer.

In this paper, the development of an integrated computer-based data-acquisition system for RES plants is described. The proposed method is based on precision electronic circuits and an easy-to-use graphical environment, based on the LABVIEW program, for processing, displaying and storing the collected data. The system operator can easily process the measured parameters using any LABVIEW built-in function available. The proposed architecture has the advantages of rapid development and flexibility in the case of changes, while it can be easily extended for controlling the RES system operation.

References

[1] Blaesser G. PV system measurements and monitoring: the European experience. Solar Energy Mater. Solar Cells 1997;47:167–76.
[2] Wilshaw A, Pearsall N, Hill R. Installation and operation of the first city center PV monitoring station in the United Kingdom. Solar Energy 1997;59:19–26.
[3] Kim M, Hwang E. Monitoring the battery status for photovoltaic systems. J. Power Sources 1997;64:193–6.
[4] Benghanem M, Maafi A. Data acquisition system for photovoltaic systems performance monitoring. IEEE Trans. Instrument. Meas. 1998;47:30–3.
[5] Benghanem M, Arab AH, Mukadam K. Data acquisition system for photovoltaic water pumps. Renewable Energy 1999;17:385–96.
[6] Mukaro R, Carelse XF. A microcontroller-based data acquisition system for solar radiation and environmental monitoring. IEEE Trans. Instrument. Meas. 1999;48:1232–8.
[7] Mukaro R, Carelse XF, Olumekor L. First performance analysis of a silicon-cell microcontroller-based solar radiation monitoring system. Solar Energy 1998;63:313–21.
[8] Lundqvist M, Helmke C, Ossenbrink HA. ESTI-LOG PV plant monitoring system. Solar Energy Mater. Solar Cells 1997;47:289–94.
[9] Wichert B, Dymond M, Lawrance W, Friese T. Development of a test facility for photovoltaic–diesel hybrid energy systems. Renewable Energy 2001;22:311–9.
[10] Krauß A, Weimar U, Gopel W. LabView for sensor data acquisition. Trends Anal. Chem. 1999;18:312–8.
[11] Duryea S, Islam S, Lawrance W. A battery management system for stand alone photovoltaic energy systems. In: Proceedings of 34th Annual Meeting of the IEEE Industry Applications Conference. 1999. p. 2649–54.